The Astrophysical Journal, 628:811–816, 2005 August 1

THE HERBIG Ae STAR HD 163296 IN X-RAYS

Douglas A. Swartz,[1] Jeremy J. Drake,[2] Ronald F. Elsner,[3] Kajal K. Ghosh,[1] Carol A. Grady,[4] Edward Wassell,[5] Bruce E. Woodgate,[6] and Randy A. Kimble[6]

Received 2004 August 12; accepted 2005 March 1

ABSTRACT

Chandra X-ray imaging spectroscopy of the nearby Herbig Ae star HD 163296 at 100 AU angular resolution is reported. A pointlike, soft ($kT \sim 0.5$ keV), emission-line source is detected at the location of the star with an X-ray luminosity of 4×10^{29} ergs s^{-1} ($\log L_X/L_{bol} = -5.48$). In addition, faint emission along the direction of a previously detected Lyα-emitting jet and Herbig-Haro outflow may be present. The relatively low luminosity, lack of a hard spectral component, and absence of strong X-ray variability in HD 163296 can be explained as originating from optically thin shock-heated gas accreting onto the stellar surface along magnetic field lines. This would require a (dipole) magnetic field strength at the surface of HD 163296 of at least $\sim$100 G and perhaps as high as several kG. HD 163296 joins the T Tauri star TW Hya in being the only examples known to date of pre–main-sequence stars whose quiescent X-ray emission appears to be completely dominated by accretion.

Subject headings: stars: emission-line, Be — stars: individual (HD 163296) — stars: pre–main-sequence — X-rays: stars

1. INTRODUCTION

The Herbig Ae/Be stars (Herbig 1960) are the more massive counterparts of T Tauri stars. They are characterized by a strong IR excess, emission lines, and luminosity class III–V (Waters & Waelkens 1998). Herbig Ae/Be stars represent an important link between high-mass stars that evolve directly from embedded protostars to the zero-age main sequence (ZAMS; the onset of core H burning) and low-mass stars that stop accreting before reaching the main sequence and that can be observed in this hydrostatic pre–main-sequence phase (Appenzeller 1994).

Herbig Ae stars are often strong X-ray emitters with luminosities of order 10^{29}–10^{32} ergs s^{-1} (e.g., Hamaguchi et al. 2002, 2005). This high level of activity is possibly linked to the presence of an accretion disk and is probably ultimately driven by magnetic fields. However, the origin of magnetic fields in Herbig Ae stars is unknown. Main-sequence A stars lack the thick surface convection zones (Gilliland 1986) of late-type stars (and their T Tauri progenitors) that drive magnetic dynamo activity and power X-ray–emitting chromospheres and hot coronae. Hence, they are weak X-ray emitters (Simon et al. 1995; Linsky 2003) or even X-ray dark (Schmitt 1997). Perhaps field generation in Herbig Ae stars is not through the solar-type α-Ω dynamo mechanism but from compression of interstellar cloud fields in the initial collapse (Dudorov et al. 1989), induced by deuterium-shell burning during contraction toward the main sequence (Palla & Stahler 1993), or generated via internal differential rotation during an early accretion phase (Tout & Pringle 1995). Such fields may decay rapidly through turbulent magnetic diffusivity as the radiative core develops and only be present in the youngest Herbig Ae stars.

In analogy to T Tauri stars, whose X-ray activity is also often much greater than in evolved stars of similar mass, perhaps circumstellar material allows other magnetic configurations such as star-disk and disk-disk fields to generate the strong flares, hard X-ray emission, and high X-ray luminosity seen in some intermediate-mass Herbig Ae systems. Energetic reconnection flares may arise at the corotation interface between dipole stellar fields and the inner disk (Hayashi et al. 1996; Shu et al. 1994; Birk et al. 2000) or through differential rotation of the field-threaded disks themselves (e.g., Romanova et al. 1998). Magnetic fields are believed to regulate protostellar collapse through ambipolar diffusion, to funnel accretion from the disk, and to transfer disk orbital motion to collimated outflows (see Feigelson & Montmerle [1999] for a review).

HD 163296 is a nearby (122 pc) Herbig Ae star (A1 Ve, $A_V = 0.25$ mag) with an effective temperature $T_{eff} = 9300$ K, luminosity $\log (L_*/L_\odot) = 1.48^{+0.12}_{-0.10}$, mass $M_* = 2.3\ M_\odot$, and radius $R_* = 2.1\ R_\odot$ (van den Ancker et al. 1998). Based on its position on the H-R diagram, HD 163296 is at an age $t = 4^{+6}_{-2.5}$ Myr (van den Ancker et al. 1998), intermediate between heavily embedded pre–main-sequence A stars and near-ZAMS stars with debris disks. HD 163296 has a strong infrared excess (Hillenbrand et al. 1992; Meeus et al. 2001) and variable Balmer series emission lines (Baade & Stahl 1989; Pogodin 1994; Beskrovnaya et al. 1998), typical of the Herbig Ae class, although it has no associated molecular or dark cloud (e.g., Thé et al. 1994). The large infrared excess arises from heated, optically thick dust within a circumstellar disk (Hillenbrand et al. 1992; Meeus et al. 2001). The disk has a radius of $\sim$450 AU (3.″7) viewed at $\sim$60° inclination (Mannings & Sargent 1997; Grady et al. 2000). The time-variable double-peaked and P Cygni Balmer and UV emission-line profiles arise from a stellar wind, an extended chromosphere, and/or rotation (e.g., Catala et al. 1989). Radio continuum observations (Brown et al. 1993) of HD 163296 also suggest wind-driven mass loss. Orthogonal to the disk is an axially aligned chain of Herbig-Haro nebulae extending several arcseconds above and below the disk (Grady et al. 2000). A Lyα-bright jet extending 6″ along the southwest

[1] Universities Space Research Association, NASA Marshall Space Flight Center, SD50, Huntsville, AL 35812.
[2] Smithsonian Astrophysical Observatory, MS-3, 60 Garden Street, Cambridge, MA 02138.
[3] Space Science Department, NASA Marshall Space Flight Center, SD50, Huntsville, AL.
[4] Eureka Scientific; and Laboratory for Astronomy and Solar Physics, Code 681, NASA Goddard Space Flight Center, Greenbelt, MD 20771.
[5] Thomas Aquinas College, Santa Paula, CA; and Institute for Astrophysics and Computational Sciences, The Catholic University of America, Washington, DC 20064.
[6] NASA Goddard Space Flight Center, Code 681, Greenbelt, MD 20771.

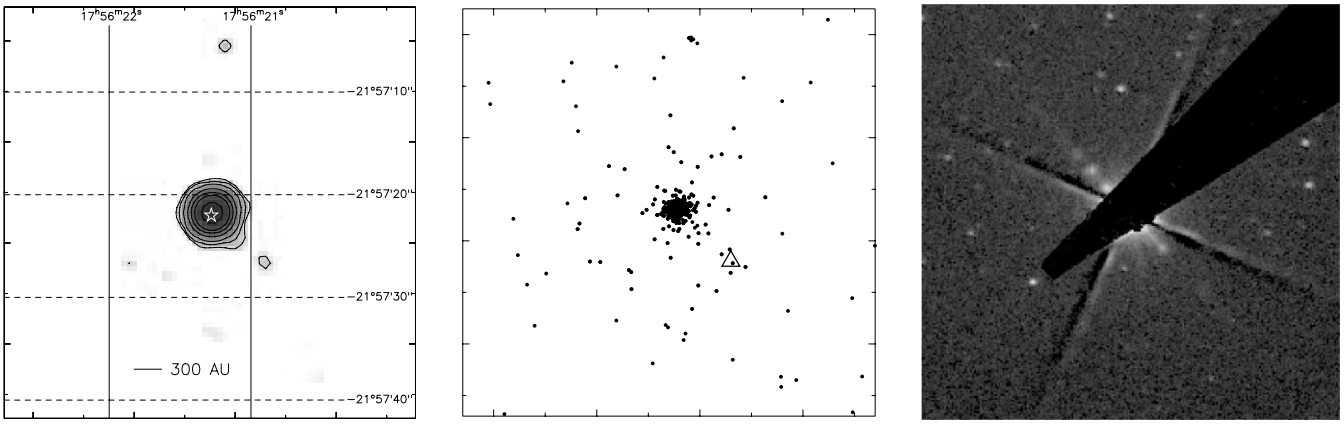

FIG. 1.—*Left*: Smoothed $40'' \times 40''$ ACIS image of the region around HD 163296 in the 0.3 to 3.0 keV bandpass obtained in 2003 August. Tick marks denote steps of 5 ACIS pixels ($0''.492$ pixel^{-1}). North is up and east is to the left. The star symbol marks the *Hipparcos* position of HD 163296. Contours denote 0.1, 0.2, 0.5, 2, 5, 10, and 30 counts pixel^{-1} levels. The lowest contour extends $>2''$ from the center of the bright source along the southwest in the direction of the Lyα jet reported by Devine et al. (2000) (P.A. $= 42^{\circ}.5 \pm 3^{\circ}.5$). The diffuse isolated feature is $\sim 7''$ from the central source and nearly along this axis. The debris disk (Mannings & Sargent 1997; Grady et al. 2000) is oriented perpendicular to the jet with radius $\sim$450 AU ($3''.7$) and inclination $\sim 60^{\circ}$. *Middle*: Individual X-ray event locations for the data shown at left. The triangle denotes the centroid of the weak diffuse feature. *Right*: $20'' \times 20''$ continuum-subtracted [S II] image obtained 2004 May. Note the occulting wedge shadow and diffraction spikes from HD 163296. The jet and knot structures are clearly visible and extend $\sim 27''$ from the star along both the jet and counterjet. The structure in the counterjet (toward the northeast) has no apparent X-ray counterparts. The optical knots have proper motions of 0.410 ± 0.005 s yr^{-1}.

arm of the Herbig-Haro flow has also been discovered (Devine et al. 2000).

HD 163296 was examined with *Chandra* in order to study the spatial distribution of the X-ray radiation from the star and circumstellar environment (§ 2) and to characterize the X-ray spectrum and light curve (§ 3). The combination of an accretion disk and jet in a relatively old Herbig Ae object, a low extinction due to a lack of association with dark clouds, the presence of Herbig-Haro objects along the jet axis, and an otherwise source-free field make HD 163296 a particularly promising object for high-resolution X-ray imaging spectroscopy. It is found that the bulk of the X-ray emission is associated with the central star and its immediate surroundings. This emission can be described as a cool, $\sim$0.5 keV, emission-line plasma with a luminosity of $\sim 4 \times 10^{29}$ ergs s^{-1} in the 0.3–3.0 keV range. There is also evidence for X-ray emission along the jet. Possible origins of the X-ray emission are discussed in § 4.

2. X-RAY IMAGE

HD 163296 was observed for 19.2 ks on 2003 August 10. The observation utilized *Chandra*'s Advanced CCD Imaging Spectrometer (ACIS) operating in 1/4 subarray, timed-exposure, imaging mode. Only the central three CCDs, S2–S4, were active during the observation, resulting in an approximately $2'.1 \times 25'.3$ image and a 0.941 s frame time. This configuration was chosen to provide the highest integrity image by minimizing event pileup. Randomization of event locations at the subpixel level, part of the standard data processing pipeline, was removed by reprocessing the data. Standard *ASCA* grade 02346 events in the 0.3–8.0 keV energy range were included in the analysis.

Nine weak pointlike sources (each with 9–17 counts detected, corresponding to signal-to-noise ratios of 2.5–3.6) and one bright source (1131 counts) were detected in the field. One of the weak sources is $0''.20$ offset in R.A. from a source in the Two Micron All Sky Survey (2MASS) All-Sky Data Release catalog. This is comparable to the estimated statistical uncertainty in the X-ray position of that source. No other astrometric catalog matches were found for any of the other weak X-ray sources. The bright source is offset $-0''.26$ in declination, $0^{s}.00$ in R.A., from the *Hipparcos* position of HD 163296 extrapolated to the time of the X-ray observation ($17^{h}56^{m}21^{s}.28524$, $-21^{\circ}57'22''.0248$). This is within the 1 σ nominal *Chandra* absolute pointing uncertainty[7] of $0''.38$ and infers the X-ray emission is from HD 163296 and not from a nearby late-type companion.

Hubble Space Telescope (*HST*) observations also place tight constraints on a potential companion. Late-type companions produce conspicuous diffraction patterns in STIS chronographic imagery with spatial intensity profiles distinctly different from those of early A stars (see Grady et al. [2004] for examples in the field of HD 104237). STIS imagery of HD 163296 shows no evidence for a late-type companion beyond $0''.05$ of HD 163296. In addition, long-slit STIS spectra of HD 163296 are characteristic of chromospheric and transition region spectra of early-type stars and display the spatial profile of an unresolved point source. The emission-line features seen in these and in *FUSE* data (Grady et al. 2005) are uniformly broad and often double-peaked. Such features are characteristic of Herbig Ae stars and are much broader than those of late-type stars; even rapid rotators like the M1 Ve star AU Mic (Pagano et al. 2000; Robinson et al. 2001). Both line and UV/FUV emission are spatially coincident, at the resolution of *HST*, with the photosphere of HD 163296. In particular, emission associated with transition region temperature plasma, N V and O VI, originate on the rapidly rotating HD 163296 rather than on a more slowly rotating, but otherwise unseen, late-type companion. We conclude that there are no late-type stellar companions to HD 163296.

The central $40'' \times 40''$ region of the X-ray image is shown in the left panel of Figure 1. A nearest-neighbor (boxcar) smoothing has been applied to the image, and contours have been added to emphasize the weak extension from the source toward the southwest and diffuse structure located $\sim 7''$ from the bright source along this jet axis. The roll angle for the observation is $268^{\circ}.5$, placing any readout streak along an east-west line (left-right in the figures) through the bright source or roughly 45° from the jet axis. Thus, there is no contribution to the X-ray extension along the jet axis from the readout streak. The center

[7] See http://cxc.harvard.edu/cal/ASPECT/celmon.

panel of Figure 1 shows the positions of the individual X-ray events with the location of the weak diffuse feature marked.

The right panel of Figure 1 shows, for comparison, a portion of an ultra-narrowband [S II] image of HD 163296 taken on 2004 May 17 using the Goddard Fabry-Perot (GFP) instrument and a coronagraphic wedge to occult the central starlight on the 3.5 m telescope at the Apache Point Observatory in Sunspot, New Mexico. The image was constructed from an on-band image centered at 6724 Å with a 12 Å FWHM (or 540 km s^{-1}, thereby sampling both the jet at -300 km s^{-1} and the counterjet at +340 km s^{-1}) from which an off-band image centered at 6750 Å with a 12 Å FWHM was subtracted. Both images are 900 s exposures taken under conditions of 1.″5 seeing. The GFP field of view is a circular aperture of 3.′7 diameter and the CCD plate scale is 0.″366 pixel^{-1}. A $40'' \times 40''$ subimage of the full GFP image centered on the star is shown. Herbig-Haro knots associated with the jet and counter jet of HD 163296 are visible in the raw GFP observation and can be traced out to $\pm 27''$ from the star after subtraction of the off-band image. The knots in both the jet and counterjet were measured at S/N = 10. The weak X-ray feature does not overlap any of the optical knots when their positions are devolved to the time of the X-ray observation using the known knot proper motions.

The spatial distribution of the X-ray events from the central portion of HD 163296 was compared to a model point-spread function (PSF) to test for possible source extension. The model PSF was generated using the *Chandra* Ray Tracer (ChaRT) Web-based interface[8] to the SAOsac ray-trace code using the best-fit single-kT model spectrum ($kT \sim 0.5$ keV, § 3). The radial profile (averaged over azimuth) of the data shows a slight excess above the model PSF in an annulus between 0.5 and ~2.″5 of the emission peak. However, the ray-trace software does not account for spacecraft dither and the observed excess is consistent with this model limitation. Therefore, except for emission along the jet, there is no conclusive evidence that the bright source is extended.

3. X-RAY SPECTRA AND TIMING

3.1. *HD 163296*

A time-dependent gain[9] correction was applied to the event file. The spectrum was then extracted from a 2 pixel–radius region about the center of the bright source. Corresponding redistribution matrix and auxiliary response files were generated using CXC/CIAO tools (ver. 2.3). Models were fit to the spectrum using the XSPEC (ver. 11.2) spectral-fitting package. The `acisabs` multiplicative absorption model[10] was included to account for the temporal decrease in low-energy sensitivity of ACIS. The C-statistic fit-minimization algorithm was used to determine the best-fit parameters for the unbinned data.

Figure 2 shows the spectrum, model, and fit residuals for an absorbed variable-abundance (`vmekal`) emission-line model (C-statistic 214.5 for 184 spectral bins). For display purposes, up to five channels have been combined to achieve a minimum 5 σ significance. The parameter estimates and 90% confidence ranges for this model are: hydrogen column density, $N_{\rm H}/10^{20} = 7.62 \pm 1.85$ cm^{-2}; plasma temperature, $kT = 0.49 \pm 0.03$ keV; and emission measure, EM $= (1.1 \pm 0.3) \times 10^{53}$ cm^{-3}.

The metal abundances were allowed to vary in the model fits but were restricted to preserve solar ratios for certain element

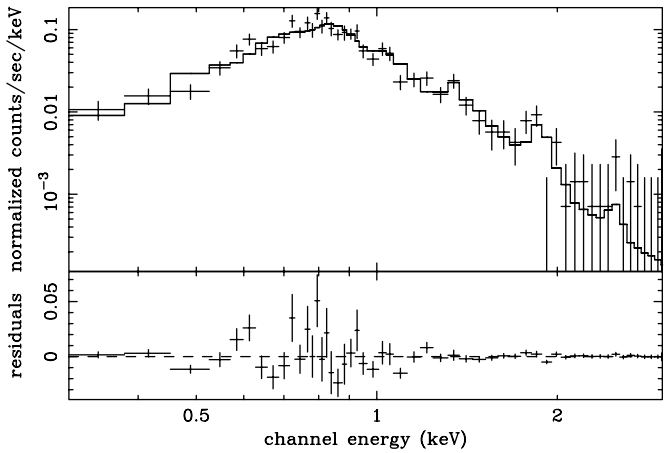

FIG. 2.—*Top*: Observed spectrum of HD 163296 (*symbols*) and best-fit single-temperature thermal emission-line (`vmekal`) model (*solid line*). *Bottom*: Fit residuals.

groups whose first ionization potentials (FIPs) are similar (to allow for possible FIP-based chemical fractionation commonly observed in late-type stellar coronae) and whose principal X-ray lines are formed at similar energies, namely, Fe-Ni-Ca, Ne-Ar, Mg-Si-S-Al-Na, and C-N-O. In this way, the number of free parameters is not excessive. The estimated best-fit metal abundances relative to solar are 0.13 ± 0.02 for the Fe group, 0.05 ± 0.05 for the Ne group, 0.18 ± 0.08 for the Mg group, and 0.25 ± 0.12 for the C group.

The best-fit value of $N_{\rm H}$ is slightly higher than that estimated from the optical extinction, $A_V = 0.25$ mag, assuming a normal extinction law (e.g., Bohlin et al. 1978). The model luminosity is 2.9×10^{29} ergs s^{-1}, corresponding to an intrinsic (absorption-corrected) luminosity of $L_{\rm X} = 4.0 \times 10^{29}$ ergs s^{-1} in the 0.3–3.0 keV energy range after correcting for the finite spectral-extraction region.

Additional models were applied to try to improve the fits and to better characterize the composition and intrinsic absorption column. These included relaxing the metal abundance restrictions in the original model, two- or three-temperature `vmekal` models, and variable-abundance absorbing columns. None of these models gave statistically significant improvements. The temperature and overall abundance are constrained by Fe, which emits numerous strong Fe XVII lines in the ~0.7–1.0 keV band. A lower-temperature plasma (in ionization equilibrium) would be needed to produce a stronger O VII triplet at ~0.57 keV and H-like N Lyα at 0.5 keV; merely increasing O and N abundances does not alter the model spectrum. If the abundances of Mg and Si are ungrouped and increased to $\sim 0.2\ Z_\odot$, then the emission at 1.35 keV (He-like Mg) and 1.84 keV (He-like Si) increases, but the fit is not statistically improved. Ne x Lyα also contributes at 1 keV, but the best-fit Ne abundance is slightly lower than that for other elements at 0.05 times the solar photospheric value.

We also investigated models with an additional thermal component, although these models resulted in no significant improvement to the model fit for the cases of both lower and higher temperatures. Forcing a component at a fixed temperature of 3 keV resulted in a contribution of at most 10% to the total flux.

Accretion shocks or shocks from a stellar wind might contribute to the observed X-ray emission from HD 163296 (§ 4.1). Models based on the physics of shock-heated plasma (e.g., `pshock` and variants following the work of Borkowski et al. 2001) were also fit to the spectrum. The resulting fits were no

[8] See http://asc.harvard.edu/chart.
[9] See http://hea-www.harvard.edu/~alexey/acis/tgain.
[10] See http://www.astro.psu.edu/users/chartas/xcontdir/xcont.html.

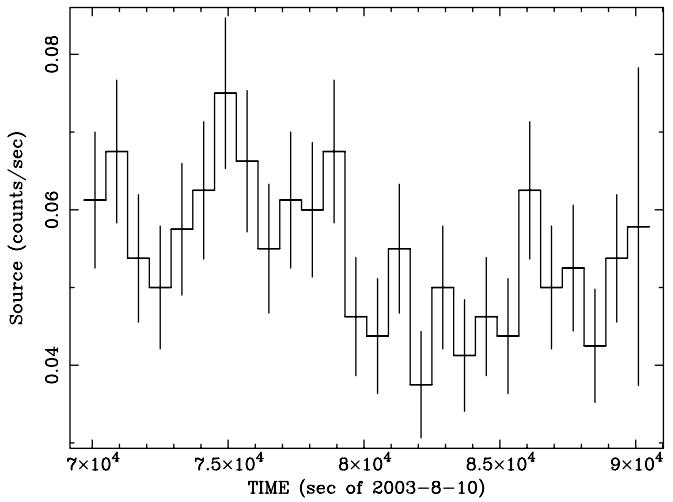

FIG. 3.—X-ray light curve of HD 163296 accumulated into 800 s bins. Data were extracted from a 2 pixel radius about the peak of the spatial distribution of events. Only events in the 0.3–3.0 keV energy range are included. The background contributes less than one event to the >1000 events in the light curve.

better than the simple absorbed `vmekal` model. The best-fit parameters of the shocked gas models (absorbing column, postshock temperature, abundance, and emission measure) were comparable to the values determined from the emission-line model.

3.2. *X-Ray Knot*

There are 5 counts in the 0.3–3.0 keV band detected within a 2.″5 radius around the position of the "knot" shown in Figure 1. This feature was not detected with our source-finding algorithm. However, the expected background is only 0.6 counts, giving a probability of 0.0004 that 5 or more Poisson-distributed counts would be detected in a given region of this size. On the entire S3 chip (in 1/4 subarray mode) there are 7 of 2625 regions of this size found to contain 5 or more counts. Thus, the distribution is not strictly Poissonian; there are also real sources present below the detect limit. There are 13.75 regions of this size within the area of the optical jet structure extending $\pm 27''$ from HD 163296. Within this area, the probability of detecting a 5 count feature in a 2.″5 radius circle is therefore 0.04.

The source counts are clustered near 0.8 keV, corresponding to the peak of the spectrum of a thermal plasma of temperature $\sim$0.3 keV when folded with the *Chandra* response. The corresponding unabsorbed X-ray luminosity of the knot is $\sim 3\times10^{27}$ ergs s^{-1}.

3.3. *HD 163296 Light Curve*

The 20 ks *Chandra* observation corresponds to about 1/3 of the rotation period of HD 163296 (van den Ancker et al. 1998). No flaring of the source was observed over the short observation. The binned light curve of HD 163296 (Fig. 3) is consistent with a constant flux ($\chi^2 = 31.9$ for 25 dof) with variations not more than $\sim$20% in amplitude. A Kolomogorov-Smirnov statistic was also computed to test the source for time variability by comparing the cumulative event arrival times binned at the frame time of 0.94 s to that expected for a steady source. This test showed the source to be marginally variable (significance level 0.006) because of the shallow dip in the light curve about midway through the observation. These two tests indicate that there is no evidence for strong variability during the observation.

4. DISCUSSION

4.1. *HD 163296*

The *Chandra* observation reveals a pointlike object within 0.″25 (30 AU) of the *Hipparcos* position of HD 163296. The X-ray luminosity is 4×10^{29} ergs s^{-1} ($\log L_X/L_{bol} = -5.48$) and the best-fit temperature is 0.5 keV (6×10^6 K). Notably, there is no evidence for the highly variable, hot ($kT \gtrsim 3$ keV), and luminous (up to $\sim10^{32}$ ergs s^{-1}) X-ray emission that has been attributed to reconnection flares in other Herbig Ae systems (e.g., Hamaguchi et al. 2002, 2005) in analogy to the late-type T Tauri stars. The spatial coincidence, X-ray spectrum, and lack of X-ray flares strongly suggest the X-ray emission is associated with HD 163296 and not with a hidden late-type companion. This conclusion is further supported by the lack of spatial and spectral evidence from *HST* STIS imagery for a late-type companion to HD 163296.

Line-driven winds also cannot account for the X-ray emission. The wind mass-loss rate is $\dot{M} \sim 10^{-15}(L_*/L_\odot)^2(M_*/M_\odot)^{-1}\ M_\odot$ yr^{-1} (see Abbott 1982). For HD 163296, $\dot{M} \sim 5.5\times10^{-13}\ M_\odot$ yr^{-1} and there is too little kinetic power in the wind, $E = (1/2)\dot{M}v^2 \sim 6\times10^{28}$ ergs s^{-1}, to account for the X-ray luminosity even if all this energy were converted to X-ray radiation through shocks.

The presence of a circumstellar debris disk, jets, and Herbig-Haro outflows are all strong indications of accretion and accretion-induced outflow in HD 163296. The luminosity released in accretion is $L_{acc} = GM_*\dot{M}/2R_*$ (excluding the portion viscously dissipated in the disk). For HD 163296, $L_{acc} = 6.6\times10^{33}\dot{M}_7$ ergs s^{-1}, where $\dot{M}_7$ is the mass accretion rate in units of $10^{-7}\ M_\odot$ yr^{-1}.

In the absence of strong magnetic fields, the accretion energy is released in an optically thick boundary layer at the surface of the star. In this case, the accretion energy radiates as a blackbody from an area $\sim 4\pi R_* H$, where $H \sim 0.1R_*$ is the height of the emission region (Popham et al. 1993), with a temperature $T \sim (GM_*\dot{M}/8\pi R_*^2 H\sigma)^{1/4}$ or $\sim 7900\dot{M}_7^{1/4}$ K for HD 163296. Boundary layers will therefore be copious UV emitters but cannot account for the X-ray spectrum of HD 163296.

Alternatively, the inner regions of the disk could be disrupted by a magnetic field associated with the accreting star. In this case, disk material couples to the field lines and is channeled onto small regions near the magnetic poles at an angle nearly normal to the stellar surface (Königl 1991; see, e.g., von Rekowski & Brandenburg [2004] for a more recent study). Accreted material is strongly shocked on impact. Applying the jump conditions for a shock perpendicular to the flow implies a postshock temperature $T_s = 3GM_*\mu m_p/8kR_*$ where $\mu = 0.6$ for ionized solar abundances, m_p is the proton mass, and the velocity just upstream of the shock is approximately the free-fall value, $v_{ff} = (2GM_*/R_*)^{1/2}$, at the surface. For HD 163296, $T_s \sim 5.7\times10^6$ K—consistent with the observed X-ray temperature.

If the accretion rate is high, however, then the stream can be of sufficiently high density that it will penetrate the stellar photosphere. Much of the X-ray radiation is then attenuated by preshock gas within the accretion flow or reprocessed within the stellar photosphere (e.g., Ulrich 1976; Stahler et al. 1980; Lamzin 1995, 1999; Calvet & Gullbring 1998; Drake 2004). The radiation field will become optically thick with an effective temperature of $T \sim (GM_*\dot{M}/4\pi R_*^3 f\sigma)^{1/4}$, where f is the fraction of the surface area covered by the accretion stream. For $f = 0.06$ (Shang et al. 2002), the effective temperature for HD 163296 is only $\sim 6000\dot{M}_7^{1/4}$ K.

The depth in the atmosphere at which the accretion shock will form is given by the balance between the ram pressure of the stream, $p_{\rm ram} = 2\dot{M}v_{\rm ff}/4\pi R_*^2 f$, and the photospheric gas pressure. For typical gas pressures of a few times 10^2–10^3 dyn cm^{-2}, the mass accretion rate must be below $\dot{M}_7 \sim 0.1$ for the X-ray–emitting shock to lie either above or only partially within photospheric layers. For significantly lower filling factors of less than 1% favored by some analyses of accreting T Tauri stars (e.g., Calvet & Gullbring 1998), the X-ray shock can remain completely buried in the photosphere even for accretion rates as low as $\dot{M}_7 \sim 0.01$. Thus, the observed X-rays from HD 163296 can only be consistent with an accretion scenario if the shocked material lies above, or at very shallow depths within, the photosphere and this occurs only for accretion rates below $\sim 10^{-8}\ M_\odot$ yr^{-1}.

The lower limit to the accretion rate obtained by assuming all the accretion luminosity emerges as X-ray radiation is only $\dot{M}_7 \sim 6\times10^{-5}$ or $\dot{M} \sim 6\times10^{-12}\ M_\odot$ yr^{-1}. At such a low rate most of the accretion luminosity should be observed in X-rays for plausible ranges of filling factor. The actual accretion rate, however, must be higher as only a fraction of the available energy emerges in X-rays and a portion of the accretion energy undoubtedly drives the observed jets and Herbig-Haro outflows from HD 163296.

This scenario also requires a stellar magnetic field. For steady state accretion, the disk is disrupted by the stellar magnetic field at a radius, R_M, roughly the corotation radius where the Keplerian angular velocity in the disk equals the angular velocity at the stellar surface (e.g., Shu et al. 1994). For HD 163296, this corresponds to $R_M = 10.6R_*$ (adopting $v \sin i \sim 120$ km s^{-1} as tabulated by van den Ancker et al. 1998).

This radius is where the torque exerted by the magnetic field on the disk approximately equals the viscous torque in the disk and is given by the Alfvén radius, $r_{\rm A}$, for a dipole field. The Alfvén radius can be expressed in terms of the magnetic field strength at the stellar surface, the stellar mass, radius, and accretion rate (e.g., Frank et al. 1985). For HD 163296, $r_{\rm A} = 7.2\times10^9\dot{M}_7^{-2/7}B_*^{4/7}$. Assuming $r_{\rm A} = R_M$ results in a value of $B_* \sim 10\dot{M}_7^{1/2}$ kG for the surface field strength for HD 163296.

For the minimal accretion rate of $\dot{M}_7 \sim 6\times10^{-5}$, the required magnetic field strength is only $\sim$80 G. Higher magnetic fields, of order 500 G, have been invoked to explain confinement of plasma during strong flares observed from the Herbig Ae star V892 (Giardino et al. 2004) and the Herbig Be star MCW 297 (Hamaguchi et al. 2000). Very recently, Hubrig et al. (2004) presented evidence for (longitudinal) fields of several hundred gauss on Herbig Ae stars—values consistent with surface field strengths of up to 2 kG measured from many classical T Tauri stars (e.g., Guenther et al. 1999; Johns-Krull et al. 1999). Theoretically, these are plausible relic field strengths for a young star (see references in § 1) and imply accretion rates of order $\dot{M}_7 \sim 10^{-3}$ or higher. Combining this with the simplistic arguments based on one-dimensional shocks given above suggests an accretion rate of $\dot{M} \sim 10^{-9\pm1}\ M_\odot$ yr^{-1}, tuned such that the great majority of the X-ray emission is reprocessed within the photosphere and such that only on the order of 1% or less is actually observed at X-ray wavelengths. This rate is comparable to those reported in the literature. Gullbring et al. (1998) report rates as low as a few times $10^{-10}\ M_\odot$ yr^{-1} for a number of T Tauri stars while Calvet et al. (2004) find rates of a few times $10^{-8}\ M_\odot$ yr^{-1} for young 1–3 $M_\odot$ T Tauri (pre-Herbig Ae) stars.

The accretion rate and magnetic field strength of HD 163296 can be better determined when the contributions from the observed mass outflow are properly accounted for in the overall energy budget. Until then we conclude that the X-ray emission from HD 163296 is most consistent with an optically thin shocked accretion flow confined by a stellar (dipole) magnetic field of unknown origin. The X-ray data do not require a late-type companion be present and are in fact inconsistent with the hotter coronal temperatures (10^7 K) that typically characterize active late-type stellar coronae. A high accretion rate and strong magnetic field are also not required, although they would ease difficulties that are otherwise present in explaining the accretion-driven X-rays using simplistic accretion shock models.

HD 163296 is remarkable in being in a class of a very few pre–main-sequence stars whose observed X-ray emission has such a cool characteristic temperature that it can be entirely explained in terms of accretion. Accreting T Tauri stars generally exhibit X-ray emission characteristic of plasma at temperatures of 10^7 K or higher, similar to very active late-type stars. There is to our knowledge only one other pre–main-sequence object whose X-ray emission is also accretion-dominated: the nearby T Tauri star TW Hya (e.g., Kastner et al. 2002). Other phenomena such as giant outbursts have also been observed (Kastner et al. 2004) that signal the onset of mass accretion at rates much higher than required to explain the X-ray behavior reported here for HD 163296.

4.2. *X-Ray Knot*

Detection of X-ray emission associated with Herbig-Haro objects is not unprecedented. These shock-heated objects are formed when supersonic outflow collides with ambient material or previous ejecta (e.g., Schwartz 1983). Pravdo et al. (2001) report X-ray emission from HH 2 in Orion at the level of 5×10^{29} ergs s^{-1}, and Favata et al. (2002) estimate a luminosity of $\sim3\times10^{29}$ ergs s^{-1} from Herbig-Haro knots in the protostellar jet of L1551 IRS5. The luminosity deduced here for the isolated knot in the southwest jet is far less than these values yet is not unreasonable for an adiabatic shock. From the analytic model of Raga et al. (2002), the luminosity is $L \sim 1.8\times10^{29}(n/100)^2(r/10^{16})^3(v/100)$ ergs s^{-1} for a shock velocity v km s^{-1}, a preshock density n cm^{-3}, and a bow shock length scale r cm. For a shock velocity equal to that of the jet ($\sim$350 km s^{-1}), a typical preshock density ($\sim$100 cm^{-3}), and a bow shock length scale on the order of the optical size of the knot ($\sim10^{15}$ cm), the free-free luminosity is $\sim6\times10^{26}$ ergs s^{-1}. This is comparable to the value of $\sim3\times10^{27}$ ergs s^{-1} estimated here for the emission feature along the HD 163296 jet axis.

Support for this research was provided in part by NASA/*Chandra* award number GO3-4006X to D. A. S. Optical data are based on observations made with the Apache Point Observatory 3.5 m telescope, which is owned and operated by the Astrophysical Research Consortium. The Goddard Fabry-Perot (GFP) is supported by NASA RTOP 188-01-22. Data analysis facilities for the GFP are provided by the Laboratory for Astronomy and Solar Physics at NASA GSFC. Use was also made of *Hubble Space Telescope* observations obtained as part of HST-GTO-7065, HST-GTO-8065, and HST-GTO-8801. Support for the STIS IDT was provided by NASA Guaranteed Time Observer (GTO) funding to the STIS Science Team in response to NASA A/O OSSA-4-84 through the *Hubble Space Telescope* Project at Goddard Space Flight Center. C. A. G. was supported through NASA PO 70789-G and NASA PR 4200048153 to Eureka Scientific.

REFERENCES

Abbott, D. C. 1982, ApJ, 259, 282
Appenzeller, I. 1994 in ASP Conf. Ser. 62, The Nature and Evolutionary Status of Herbig Ae/Be Stars, ed. P. S. Thé, M. R. Perez, & E. P. J. van den Heuvel (San Francisco: ASP), 12
Baade, D., & Stahl, O. 1989, A&A, 209, 268
Beskrovnaya, N. G., Pogodin, M. A., Yudin, R. V., Franco, G. A. P., Vieira, S. L. A., & Evans, A. 1998, A&AS, 127, 243
Birk, G. T., Schwab, D., Wiechen, H., & Lesch, H. 2000, A&A, 358, 1027
Bohlin, R. C., Savage, B. D., & Drake, J. F. 1978, ApJ, 224, 132
Borkowski, K. J., Lyerly, W. J., & Reynolds, S. P. 2001, ApJ, 548, 820
Brown, D. A., Pérez, M. R., & Yusef-Zadeh, F. 1993, AJ, 106, 2000
Calvet, N., & Gullbring, E. 1998, ApJ, 509, 802
Calvet, N., Muzerolle, J., Briceño, C., Hernández, J., Hartmann, L., Saucedo, J. L., & Gordon, K. D. 2004, AJ, 128, 1294
Catala, C., Simon, T., Praderie, F., Talavera, A., Thé, P. S., & Tijn A Djie, H. R. E. 1989, A&A, 221, 273
Devine, D., et al. 2000, ApJ, 542, L115
Drake, J. J. 2005, in Cool Stars, Stellar Systems and the Sun: 13th Cambridge Workshop, ed. F. Favata & G. Hussain (ESA-SP; Noordwijk: ESA), in press
Dudorov, A. E., Krivodubskii, V. N., Ruzmaikina, T. V., & Ruzmaikin, A. A. 1989, Soviet Astron., 33, 420
Favata, F., Fridlund, C. V. M., Micela, G., Sciortino, S., & Kaas, A. 2002, A&A, 386, 204
Feigelson, E. D., & Montmerle, T. 1999, ARA&A, 37, 363
Frank, J., King, A. R., & Raine, D. J. 1985, Accretion Power in Astrophysics (Cambridge: Cambridge Univ. Press)
Giardino, G., Favata, F., Micela, G., & Reale, F. 2004, A&A, 413, 669
Gilliland, R. L. 1986, ApJ, 300, 339
Grady, C. A., Williger, G. M., Bouret, J.-C., Roberge, A., Sahu, M., & Woodgate, B. 2005, in ASP Conf. Ser., Astrophysics in the Far Ultraviolet, ed. B.-G. Anderssen, G. Sonneborn, & W. Moos (San Francisco: ASP), in press
Grady, C. A., et al. 2000, ApJ, 544, 895
———. 2004, ApJ, 608, 809
Guenther, E. W., Lehmann, H., Emerson, J. P., & Staude, J. 1999, A&A, 341, 768
Gullbring, E., Hartmann, L., Briceño, C., & Calvet, N. 1998, ApJ, 492, 323
Hamaguchi, K., Koyama, K., Yamauchi, S., & Terada, H. 2002, in ASP Conf. Ser. 277, Stellar Coronae in the *Chandra* and *XMM-Newton* Era, ed. F. Favata & J. J. Drake (San Francisco: ASP), 193
Hamaguchi, K., Terada, H., Bamba, A., & Koyaman K. 2000, ApJ, 532, 1111
Hamaguchi, K., Yamauchi, S., & Koyama, K. 2005, ApJ, 618, 360
Hayashi, M. R., Shibata, K., & Matsumoto, R. 1996, ApJ, 468, L37
Herbig, G. H. 1960, ApJS, 4, 337
Hillenbrand, L. A., Strom, S. E., Vrba, F. J., & Keene, J. 1992, ApJ, 397, 613
Hubrig, S., Schöller, M., & Yudin, R. V. 2004, A&A, 428, L1
Johns-Krull, C. M., Valenti, J. A., & Koresko, C. 1999, ApJ, 516, 900
Kastner, J. H., Huenemoerder, D. P., Schulz, N. S., Canizares, C. R., & Weintraub, D. A. 2002, ApJ, 567, 434
Kastner, J. H., et al. 2004, Nature, 430, 429
Königl, A. 1991, ApJ, 370, L39
Lamzin, S. A. 1995, A&A, 295, L20
———. 1999, Astron. Lett. 25, 430
Linsky, J. L. 2003, Adv. Space Res., 32, 917
Mannings, V., & Sargent, A. I. 1997, ApJ, 490, 792
Meeus, G., Waters, L. B. F. M., Bouwman, J., van den Ancker, M. E., Waelkens, C., & Malfait, K. 2001, A&A, 365, 476
Pagano, I., Linsky, J. L., Carkner, L., Robinson, R. D., Woodgate, B., & Timothy, G. 2000, ApJ, 532, 497
Palla, F., & Stahler, S. W. 1993, ApJ, 418, 414
Pogodin, M. A. 1994, A&A, 282, 141
Popham, R., Narayan, R., Hartmann, L., & Kenyon, S. 1993, ApJ, 415, L127
Pravdo, S. H., Feigelson, E. D., Garmire, G., Maeda, Y., Tsubol, Y., & Bally, J. 2001, Nature, 413, 708
Raga, A. C., Noriega-Crespo, A., & Velázquez, P. F. 2002, ApJ, 576, L149
Robinson, R. D., Linsky, J. L., Woodgate, B. E., & Timothy, J. G. 2001, ApJ, 554, 368
Romanova, M. M., Ustyugova, G. V., Koldoba, A. V., Chechetkin, V. M., & Lovelace, R. V. E. 1998, ApJ, 500, 703
Schmitt, J. H. M. M. 1997, A&A, 318, 215
Schwartz, R. D. 1983, ARA&A, 21, 209
Shang, H., Glassgold, A. E., Shu, F. H., & Lizano, S. 2002, ApJ, 564, 853
Shu, F., Najita, J., Ostriker, E., Wilkin, F., Ruden, S., & Lizano, S. 1994, ApJ, 429, 781
Simon, T., Drake, S. A., & Kim, P. D. 1995, PASP, 107, 1034
Stahler, S. W., Shu, F. H., & Taam, R. E. 1980, ApJ, 241, 637
Thé, P. S., de Winter, D., & Pérez, M. R. 1994, A&AS, 104, 315
Tout, C. A., & Pringle, J. E. 1995, MNRAS, 272, 528
Ulrich, R. K. 1976, ApJ, 210, 377
van den Ancker, M. E., de Winter, D., & Tijn A Djie, H. R. E. 1998, A&A, 330, 145
von Rekowski, B., & Brandenburg, A. 2004, A&A, 420, 17
Waters, L. B. F. M., & Waelkens, C. 1998, ARA&A, 36, 233